ELSEVIER

Journal of Membrane Science 113 (1996) 7–20

journal of MEMBRANE SCIENCE

Controlled release of theophylline from water-swollen scleroglucan matrices

Alessandra Adrover [a,*], Massimiliano Giona [b], Mario Grassi [c], Romano Lapasin [c], Sabrina Pricl [c]

[a] *Centro di Ricerca sui Sistemi Disordinati e Frattali nell' Ingegneria Chimica Dipartimento di Ingegneria Chimica, Università di Roma "La Sapienza", Via Eudossiana 18, 00184 Roma, Italy*

[b] *Centro di Ricerca sui Sistemi Disordinati e Frattali nell' Ingegneria Chimica Dipartimento di Ingegneria Chimica, Universitá di Cagliari, Piazza d'Armi, 09123 Cagliari, Italy*

[c] *Centro di Ricerca sui Sistemi Disordinati e Frattali nell' Ingegneria Chimica Dipartimento di Ingegneria Chimica, Universitá di Trieste, Piazza Europa 1, 34127 Trieste, Italy*

Accepted 11 July 1995

Abstract

A two-phase model for diffusion and drug release through swollen polymeric matrices is presented and solved. This model explains the non-Fickian release behaviour experimentally found for the system constituted by theophylline in a water-swollen scleroglucan matrix in a slab form. The exponential nature of the temporal behaviour of the drug in the stationary phase is confirmed by means of Green function analysis. The boundary conditions deriving from the non-self-sustaining nature of the polymeric gel and from the presence of a net are investigated in detail.

Keywords: Anomalous release; Swollen gels; Two-phase modelling; Boundary condition analysis

1. Introduction

One of the open problems in controlled release analysis is the interpretation of pseudo non-Fickian kinetics in swollen hydrogels [1–4], expressed by a semiempirical power-law behaviour in the fractional solute release M_t/M_∞,

$$M_t/M_\infty \sim t^n, \quad M_t/M_\infty < 0.5. \tag{1}$$

In release structures in the swollen state, solute diffusion is not coupled to the simultaneous evolution of the gel front: the swelling degree is kept practically constant during the experiment. The interpretation of relationship (1) is not only important from the theoretical standpoint but has important consequences in the design of optimal release matrices in order to obtain matrix devices with the desired release kinetics (e.g. zero-order kinetics).

* Corresponding author.

SSDI 0376-7388(95)00289-8

In a previous article [5] we analyzed the role of the disordered structure of a matrix on the release kinetics [6] and proposed a two-phase model to explain the apparent exponent n greater than $1/2$. The reason for the introduction of a two-phase model is related to the presence of hinderance or field effects between the solute and polymeric matrix, which can be expressed macroscopically in terms of irreversible adsorption kinetics.

In this article we present and analyze the experimental results of the release of theophylline from water-swollen scleroglucan matrices by comparing these data with the prediction of the kinetic model proposed in [5].

The article is organized as follows. First we evaluate the effective diffusion coefficient of theophylline in scleroglucan matrices. Then we consider the influence of the experimental apparatus on the boundary conditions induced by the presence of a wire gauze to sustain the gel. General criteria are proposed and it is shown that the wire gauze introduces mixed boundary conditions which, for the experimental conditions under investigation, can be neglected and therefore do not modify the assumption of perfect sink conditions.

We then discuss in detail the application of the two-phase model to the experimental results of theophylline in water-swollen scleroglucan. The model is also compared with other literature data [3]. A short-cut method is proposed for evaluating the kinetic rate k (describing in the two-phase model the irreversible release from the gel phase to the sol phase) from the value of the diffusivity and of the exponent n. Black-box analysis of the release data based on the application of the Green function method confirms the validity of the model proposed.

2. Experimental

2.1. Materials

The polysaccharide scleroglucan (Actigum CS11, $M_W \simeq 1.2 \times 10^6$, Mero-Russelot-Satia, France) used for hydrogel matrix formulation was supplied by Vectorpharma S.p.A., Trieste, Italy.

Theophylline ($C_7H_8N_4O_2$, $M_W = 180.17$, water solubility at 25°C = 8.3 mg/g) was chosen as a typical model drug.

For the preparation of homogeneous self-sustaining hydrogel systems, scleroglucan was slowly added to well-stirred aqueous theophylline solutions at room temperature. The systems were allowed to rest for 12 h to obtain polymer swelling and gel formation. A polymer concentration of 2% w/w was chosen to ensure the required stable gel characteristics.

2.2. Diffusion cell and drug detecting systems

The diffusion cell used in controlled-release experiments is schematically depicted in Fig. 1A. As can be seen in Fig. 1A, the diffusion cell looks like a double-walled beaker open at the top. The thickness of the gel-slab is $L = 6$ mm. The Teflon vessel containing the hydrogel, open at the top and closed with a net at the bottom, is placed at the top of the diffusion cell filled with distilled water (top configuration). The contact between hydrogel and release environment. (inner cylinder) takes place through the holes of a net. The homogeneous distribution of the drug in the release environment is ensured by a magnetic stirrer, placed at the bottom of the inner cylinder. Fig. 1B) shows a schematic diagram of the experimental setup. During each test, drug concentration in the release environment was monitored via an on-line Perkin Elmer Lambda series UV spectrophotometer (wavelength $\lambda = 217$ nm, cell path = 0.1 cm). Experimental concentration values were automatically collected with a sampling time of 10 s and stored by a computerized system. A peristaltic pump was used for system liquid circulation and a surge chamber was inserted between the diffusion cell and the pump to reduce hydrogel matrix erosion due to interface oscillation.

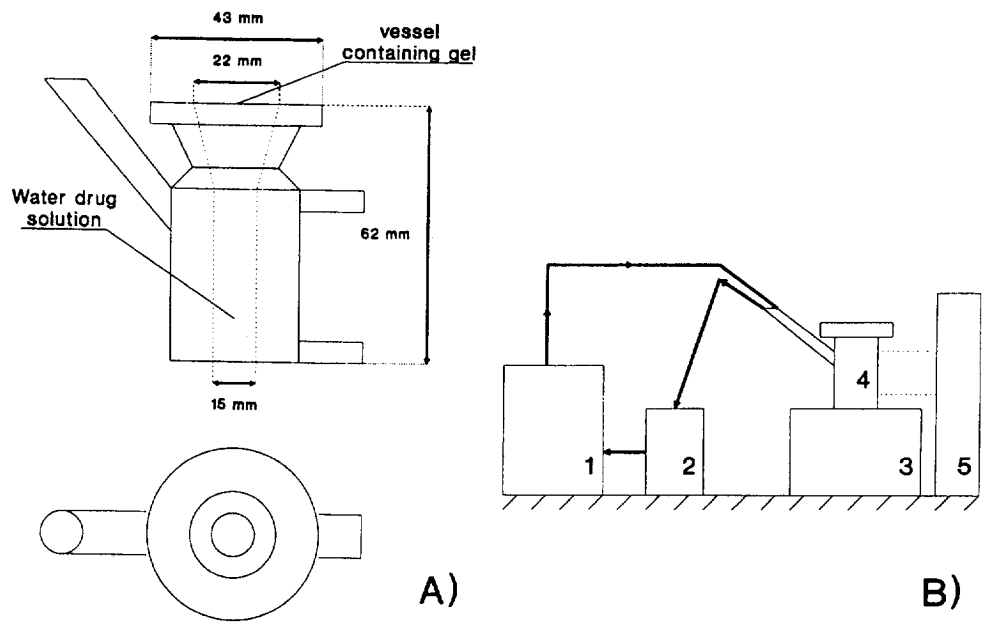

Fig. 1. (A) Schematic representation of the diffusion cell. (B) Schematic diagram of the experimental setup: (1) spectrophotometer; (2) pump; (3) magnetic stirrer; (4) diffusion cell; (5) thermostatic system.

2.3. Operating variable

The selected operation variables are reported in Table 1. A range of theophylline concentrations c_0 was chosen to investigate the effects of drug concentration on the release process. Different stirring speeds and temperature values (including the physiologically interesting values) were also adopted to check on agitation and thermal effects on the kinetics. Data reproducibility was ensured by running each experiment in triplicate.

3. Effective diffusion coefficient

Let us consider the diffusion of an initially uniformly distributed drug (theophylline) through a water-swollen polymeric (scleroglucan) non-erodible matrix in slab form under perfect sink conditions. The initial loading of the matrix is lower than the solubility limit and the degree of swelling is constant during the experiment. The simplest one-dimensional model describing the phenomenon is

$$\frac{\partial c}{\partial t} = D\frac{\partial^2 c}{\partial x^2}, \tag{2}$$

Table 1
Selected operation variables

Stirring speed	$\Omega = 100, 300, 600$ (rpm)
Concentration of theophylline in the hydrogel	$c_0 = 1.0\text{-}8.0$ (mg/g)
Temperature	$T = 20\text{-}35$ (°C)

to be solved with the initial and boundary conditions:

$$c(x,0) = c_0 \quad 0 \le x \le L, \tag{3}$$

$$\left.\frac{\partial c}{\partial x}\right|_{x=0} = 0, \quad c(L,t) = 0 \tag{4}$$

L being the thickness of the slab and D the effective diffusion coefficient of the drug in the swelling agent. The effective diffusion coefficient D takes into account the influence of the polymeric matrix on the diffusive motion of the drug in the solvent and deviates from the corresponding Stokes–Einstein diffusivity D_E by a factor G, called the accessibility factor, which macroscopically describes the steric interactions between solute and porous matrix [7]

$$D = D_E G \tag{5}$$

The solute fraction released up to time t attains the form

$$M_t/M_\infty = 1 - \frac{8}{\pi^2}\sum_{m=1}^{\infty}\frac{1}{(2m-1)^2}\exp\left[-\frac{(2m-1)^2\pi^2 Dt}{4L^2}\right] \tag{6}$$

and the effective diffusion coefficient D can be evaluated from the typical asymptotic (i.e. for large t) exponential relaxation associated with diffusive motion [5]

$$\ln(1 - M_t/M_\infty) \sim -\frac{\pi^2}{4L^2}Dt. \tag{7}$$

The value of D evaluated from Eq. (7) for the system theophylline/water-swollen scleroglucan for a fixed degree of swelling s ($s = 49$ mg H_2O/mg polymer, $c_0 = 1.0$ mg/g H_2O) is $6.0 \pm 0.7 \cdot 10^{-6}$ cm^2/s at $T = 30$°C (see Fig. 2). Fig. 3 shows the dependence of D on temperature T, in the temperature range $20 \le T \le 35$°C. It can be seen that the temperature dependence of D can be practically neglected by further considering that the variability range of D with T is of the same order of magnitude as the error in evaluating D itself.

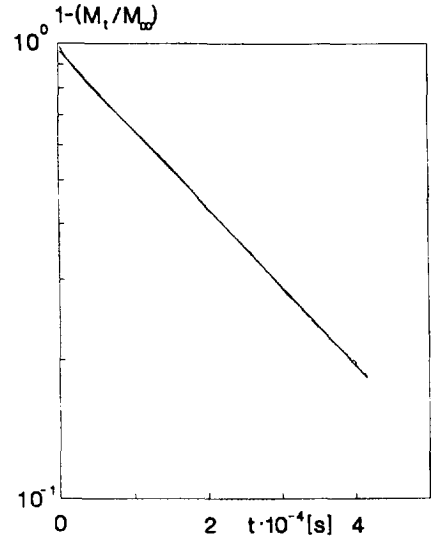

Fig. 2. Log-normal plot of $1-(M_t/M_\infty)$ vs. t ($T = 30$°C, $c_0 = 1$ mg/g H_2O). The slope of the curve is proportional to the value of the effective diffusion coefficient D [see Eq. (7)].

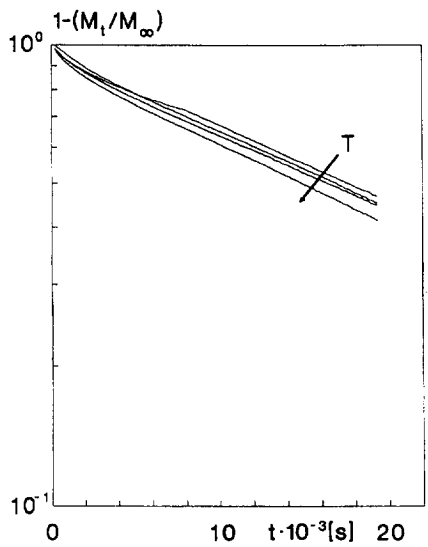

Fig. 3. Log-normal plot of $1-(M_t/M_\infty)$ vs. t for different values of the temperature T in the range $20 \leq T \leq 35$°C. The arrow indicates increasing temperature.

It is important to observe that the asymptotic scaling law (7) depends on the boundary conditions, through the value of the eigenvalue associated with the fundamental mode [Eq. (7) corresponds to burst-effect experiments [5]] and is also valid if one considers the two-phase model discussed in [5]. See section 5 for further details.

The exponential relaxation (7) in controlled-release experiments is a typical feature of constant diffusivity devices. Deviation from Eq. (7) can be obtained only if D varies significatively with time. This can happen if the degree of swelling during solute diffusion varies appreciably and if the dependence of the diffusivity on the swelling degree cannot be neglected [8,9].

4. Boundary conditions for a non-self-sustaining gel

Under our experimental conditions the diffusion cell is placed vertically and the gel slab is sustained by means of a net. It is therefore interesting to analyze the effects of the net on the boundary conditions and specifically on the assumption of perfect sink conditions. The mathematical modeling of the release should thus be modified by considering a two-dimensional simulation taking into account that the release area is distributed over a fixed number of holes.

Fig. 4 shows the proper boundary conditions to be imposed on a two-dimensional model of the diffusion experiment. The net is characterized by the ratio φ between the effective release area A_s, and the total slab surface area A, $\varphi = A_s/A$ and by the number n_o of holes into which A_s is divided.

The release kinetics still exhibits an asymptotic exponential relaxation, analogous to Eq. (7), but the prefactor of the exponential scaling, $b(\varphi, n_o)$, is modified by the boundary conditions

$$\ln(1 - M_\tau/M_\infty) \sim -b(\varphi, n_o)\tau, \quad \tau = \frac{tD}{L^2} \tag{8}$$

and depends on φ and n_o. M_τ/M_∞ is the solute fraction released up to the dimensionless time τ, obtained from the numerical solution of a two-dimensional diffusion equation analogous to Eq. (2), subjected to the boundary conditions indicated in Fig. 4. In the numerical solution of the two-dimensional diffusion model, the dimensions

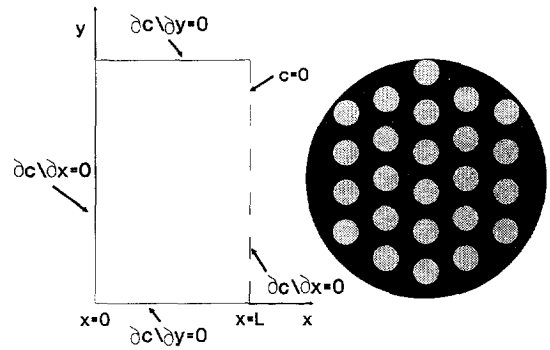

Fig. 4. Schematic representation of the proper boundary conditions to be imposed in a two-dimensional model of the diffusion phenomenon. The net has cylindrical symmetry but is modeled as a line in two-dimensional simulations. The x-axis is the transport (vertical) direction.

of the lattice representing the diffusion cell were assumed to be proportional to the corresponding dimensions of the experimental apparatus.

Fig. 5 shows that for a fixed value of φ there exists a number of holes $\bar{n}_0(\varphi)$ such that, for $n_0 \geq \bar{n}_0(\varphi)$, the prefactor $b(\varphi, n_0)$ does not depend appreciably on n_0 and practically coincides with $\lim_{\varphi \to 1} b(\varphi,n_0) = \pi^2/4$.

This implies that if $n_0 \geq \bar{n}_0(\varphi)$, the presence of the net can be neglected; that the diffusion equation can be written in one dimension and solved in a closed form by imposing perfect sink conditions and that the diffusion coefficient can be evaluated directly from Eq. (7). In our experiments $\varphi = 0.278$ and $n_0 = 356$. Consequently, from the data of Fig. 5 (for $\varphi = 0.278$) it can be seen that in our experiments perfect sink conditions can be assumed as a good approximation of the real mixed boundary conditions to be imposed at $x = L$.

5. Two-phase model

Besides the hindered effects related to the porosity and to the crosslinking of the matrix, the key problem in the kinetics of controlled release is represented by the anomalous release behaviour of gel devices showing, at intermediate time scales, an empirical power-law behaviour in the fractional solute release, Eq. (1), with an exponent n usually greater than $1/2$ (pseudo non-Fickian diffusion). Simulations of the sorption kinetics in

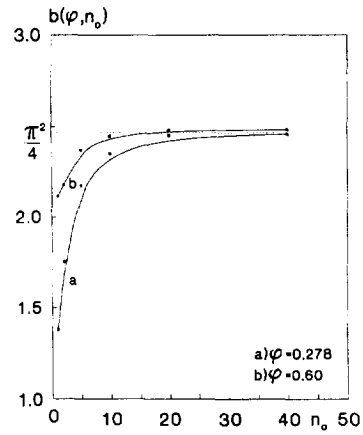

Fig. 5. $b(\varphi,n_0)$ vs. n_0 for two different values of φ. The dotted line represents $\lim_{\varphi \to 1} b(\varphi,n_0) = \pi^2/4$.

disordered models of the matrix (represented by percolation clusters) in the case both of lag and burst conditions have clearly shown that an exponent n greater than $1/2$ cannot be related to the disordered geometric and topological structure of the matrix [5]. In our experiments erosion effects are negligible and the diffusivity D of the theophylline is practically constant. The origin of the apparent non-Fickian behaviour should be a consequence of other kinetic mechanisms. The "anomalous" behaviour ($n > 1/2$) can be explained by including entrapping effects in the model associated with solute/polymeric matrix interactions, stemming from potential energy fields, hindered constraints or physical adsorption phenomena.

In each case, these effects can be macroscopically described by means of a two-phase kinetic model: a fraction ϵ_s of solute molecules is initially entrapped in the gel phase and irreversibly released in the sol phase in which the solute diffuses with an effective diffusion coefficient D. The dynamic equations describing this phenomenon are:

$$\frac{\partial c}{\partial t} = D\frac{\partial^2 c}{\partial x^2} - \frac{\partial q}{\partial t} \tag{9}$$

$$\frac{\partial q}{\partial t} = -kq, \tag{10}$$

where $c(x,t)$ and $q(t)$ are drug concentrations, respectively, in the sol and in the gel phases. Eqs. (9) and (10) are to be solved with the initial and boundary conditions:

$$c(x,0) = (1-\epsilon_s)c_0 \quad 0 < x < L, \quad q(0) = \epsilon_s c_0, \tag{11}$$

$$\left.\frac{\partial c}{\partial x}\right|_{x=0} = 0, \quad c(L,t) = 0. \tag{12}$$

For $\epsilon_s = 1$ the solute fraction released up to time t attains the form:

$$\frac{M_t}{M_\infty} = \sum_{m=1}^{\infty} \mu_m(t) \Big/ \sum_{m=1}^{\infty} \mu_{m\infty}, \tag{13}$$

with

$$\mu_m(t) = \begin{cases} \dfrac{1}{1-\bar{\Phi}_m^2}\left[\dfrac{1}{\bar{\Phi}_m^2}\left(1-\exp\left(-k\bar{\Phi}_m^2 t\right)\right) - \left(1-\exp(-kt)\right)\right] & \text{if } \bar{\Phi}_m^2 \neq 1 \\ 1-(1+t)\exp(-kt) & \text{if } \bar{\Phi}_m^2 = 1, \end{cases} \tag{14}$$

$$\mu_{m\infty} = \frac{1}{\bar{\Phi}_m^2}, \quad \text{for every } \bar{\Phi}_m^2, \tag{15}$$

$$\bar{\Phi}_m = \frac{(2m-1)\pi}{2}\frac{1}{\Phi}, \quad \Phi = \left(\frac{kL^2}{D}\right)^{\frac{1}{2}}, \tag{16}$$

where Φ is the Thiele modulus. Of course, the model proposed is valid if the initial loading of the gel is lower than the solubility limit.

As can be seen from Eqs. (13)–(16), the asymptotic relaxation behaviour of M_t/M_∞ is still given by Eq. (7) if $\Phi^2 > \pi^2/4$. This is usually the case, since the kinetic parameter k is much larger than the diffusive parameter D/L^2, as discussed in the next section.

Fig. 6A and B show the behaviour of M_t/M_∞ for different values of the kinetic constant k (for fixed values of $D = 6.0 \cdot 10^{-6}$ cm^2/s and $\epsilon_s = 1$). The log–log plot of the corresponding curves (Fig. 6B) indicates that the model furnishes values of the exponent n (evaluated at intermediate time scales) which cover all the

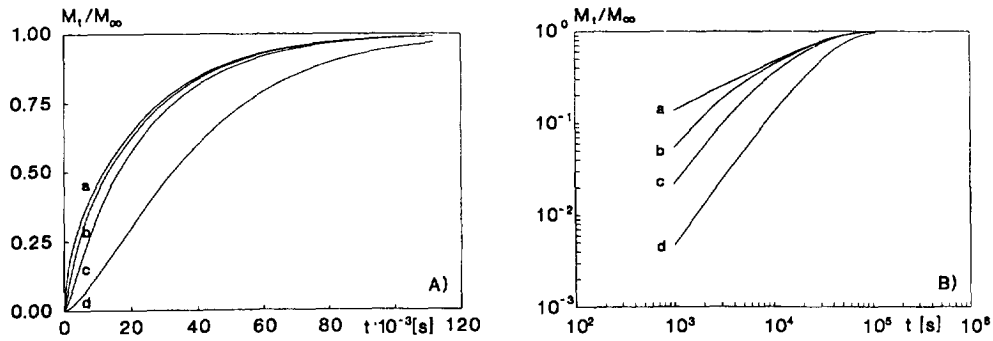

Fig. 6. (A) M_t/M_∞ vs. t for different values of the kinetic constant k; (a) $k = 1 \cdot 10^{-2}\ s^{-1}$; (b) $k = 7.5 \cdot 10^{-4}\ s^{-1}$; (c) $k = 2.5 \cdot 10^{-4}\ s^{-1}$; (d) $k = 5 \cdot 10^{-5}\ s^{-1}$. For all curves $D = 6.0 \cdot 10^{-6}\ cm^2/s$, $\epsilon_s = 1$. (B) Log–log plot of the data of Fig. 6A.

"non-Fickian" range. This is still more evident from Fig. 7A), which shows the behaviour of n vs. k for different values of D. All the curves satisfy the condition that, in the limit of large values of the Thiele modulus, the internal release kinetics is so fast with respect to the diffusive motion in the sol phase that the presence of the gel phase can be practically neglected. Consequently, the two-phase model tends to the classical diffusion model and n converges towards to 1/2.

By following the dimensionless formulation previously adopted, Eqs. (9) and (10) become

$$\frac{\partial \bar{c}}{\partial \tau} = \frac{\partial^2 \bar{c}}{\partial z^2} - \frac{\partial \bar{q}}{\partial \tau} \qquad (17)$$

$$\frac{\partial \bar{q}}{\partial \tau} = -\Phi^2 \bar{q},$$

where $\bar{c} = c/c_0$, $\bar{q} = q/q_0$, $z = x/L$, $\tau = Dt/L^2$. From the dimensionless formulation it can easily be recognized that the exponent n is a function only of the Thiele modulus (Fig. 7B). Eq. (17) and Fig. 7B make it possible to appreciate the role of the parameters entering into Eqs. (9) and (10). The diffusion coefficient D specifies the time scale of the release and can be measured from the relaxation behaviour (see section 3). The exponent n is modulated by the value of the Thiele modulus Φ^2 alone. These observations enable us to formulate a simple strategy for parameter estimation.

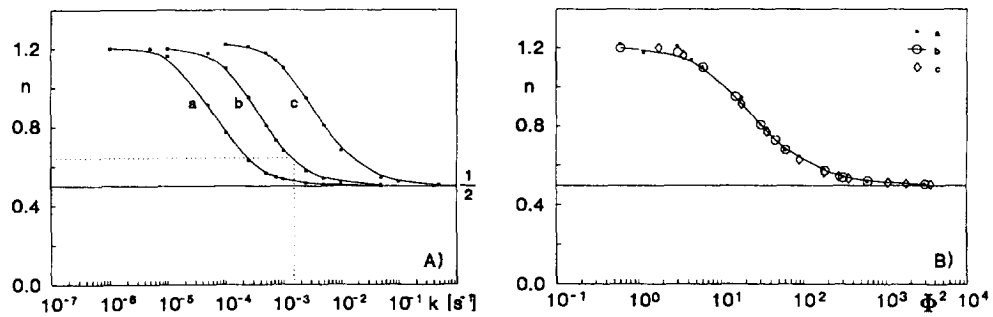

Fig. 7. (A) n vs. k for different values of D: (a) $D = 1.0 \cdot 10^{-6}\ cm^2/s$; (b) $D = 6.0 \cdot 10^{-6}\ cm^2/s$; (c) $D = 6.0 \cdot 10^{-5}\ cm^2/s$.For all curves $\epsilon_s = 1$. The dashed lines shows the evaluation of k for $n = 0.64$ and $D = 6.0 \cdot 10^{-6}\ cm^2/s$, which correspond to the parameter values experimentally found in the theophylline/water-swollen scleroglucan system. (B) n vs. Φ^2 as deduced from the data of Fig. 7A.

6. Experimental results

Fig. 8 shows in a log–log plot three experimental sorption curves of the release behaviour (under perfect sink condition) of the system theophylline/water-swollen scleroglucan at different temperatures. All the experiments were repeated three times, furnishing the same results and confirming the reproducibility of the data. The log–log scale highlighted the "anomalous behaviour", corresponding to a value of the exponent $n = 0.64 \pm 0.04$ (practically the same over the considered temperature range). As discussed above, these release profiles cannot be explained by means of a purely diffusional model and the hypothesis of solute/gel interaction should be considered.

Given the lack of information about the nature of these interactions, it is convenient to develop a short-cut procedure for the evaluation of k based on the characteristic curves of n vs. k for fixed values of D (see Fig. 7A). Once n is measured from the sorption curves and D is evaluated from relaxation data (section 3), the value of k can be readily obtained from the curve $n = n(k)$ (Fig. 7A). In all the experimental runs the value $n = 0.64$, $D = 6.0 \cdot 10^{-6}$ cm^2/s can be assumed practically constant. With these values the curve of Fig. 7A gives a value of $k = 1.5 \cdot 10^{-3}$ s^{-1}. Fig. 9A and B shows the comparison of the model with the experimental data. The agreement is fairly good. It should be also observed that, having no information about the initial division of the solute molecules between the two phases, we have assumed $\epsilon_s = 1$. The agreement of the theoretical model and the experimental results would probably be closer if the value of ϵ_s could be estimated a priori. This would involve a better understanding of the nature of the drug/matrix interactions and will be one of the future steps in our investigation.

The two-phase model can also be applied in controlled-release experiments in the presence of moderate swelling effects. Vyavahare et al. [3] present experimental data on the release of theophylline from 2-hydroxyethyl methacrylate–glycidil methacrylate (HEMA-GMA) mixtures in an acidic medium.

Fig. 10A and B show, respectively, the log–log plot of fractional release data and their reconstruction with the two-phase model. The diffusivity and the Thiele modulus were obtained by applying the methods discussed in sections 3 and 5. A review of all the experimental and model parameters is given in Table 2. As can be seen from Fig. 9B, the two-phase model proves to be in satisfactory agreement with these experimental data. The only case in which theory and experiment do not fit is that of Fig. 10B(e), for which Vyavahare et al. found the

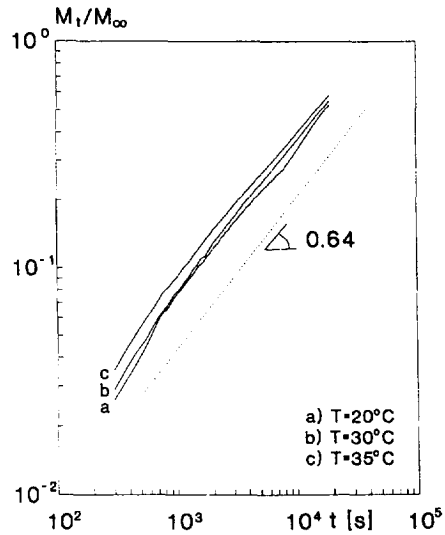

Fig. 8. Log–log plot of the experimental sorption curves (M_t/M_∞ vs. t) for different values of T. For all curves $c_0 = 1$ mg/g H_2O.

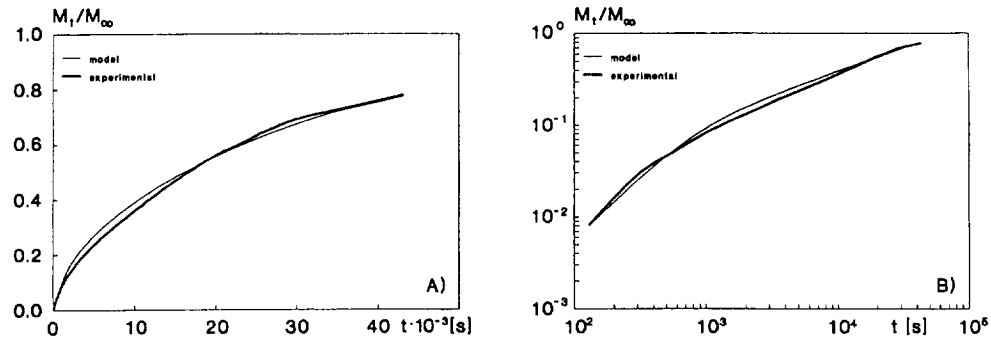

Fig. 9. Comparison of the experimental release curve ($T = 30°C$, $c_0 = 1$ mg/g H_2O) with the two-phase model predictions ($D = 6.0 \cdot 10^{-6}$ cm^2/s, $k = 1.5 \cdot 10^{-3}$ s^{-1}). (B) Log–log plot of the data of Fig. 9A.

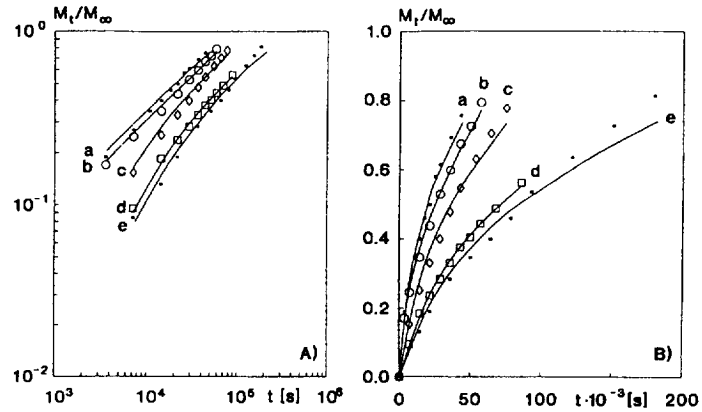

Fig. 10. Comparison of the experimental data (point) of M_t/M_∞ taken from [3] in 0.05 N H_2SO_4 at 37°C with the two-phase model predictions (curves) in log–log scale: (a) p(HEMA-15%GMA) copolymer; (b) p(HEMA-20%GMA) copolymer; (c) p(HEMA-30%GMA) copolymer; (d) p(HEMA-40%GMA) copolymer; (e) p(HEMA-50%GMA) copolymer. (B) Same data as Fig. 10A in normal scale.

maximal relative swelling degree increment $\Delta s = 0.1701$ (g H_2O/g polymer) during the release compared to the initial swelling degree $s_0 = 0.2340$ (g H_2O/g polymer). It should be observed in passing that the values of n reported in [3] are incorrectly written. The values of the exponent n reported in Table 2 correspond to the best fit of the experimental data of Fig. 10A for M_t/M_∞ up to 0.5. It should also be observed that model prediction follows the curvature effects in the log–log plot of experimental release data extremely well (see Fig. 10A). These "curvature effects" are a confirmation that the exponent n is not universal but rather a semiempirical exponent related to solute/matrix interactions.

Table 2
Review of all the experimental and model parameters evaluated from the data of Vyavahare et al. [3]

p(HEMA-GMA) copolymer GMA content (wt%)	Diffusivity D 10^7 (cm^2/s)	n (best fit)	Thiele modulus Φ^2
15	1.13 ± 0.1	0.540	275 ± 5
20	0.90 ± 0.1	0.540	275 ± 5
30	0.69 ± 0.1	0.708	49 ± 1
40	0.33 ± 0.03	0.703	49 ± 1
50	0.33 ± 0.03	0.721	46 ± 1

7. Experimental validation of two-phase model: Green function analysis

The validation of the two-phase model proposed in the previous sections can be performed by a direct analysis of the experimental data. In general, in the presence of a uniform distribution of the solute in the gel phase, it is possible to express the balance equation describing drug release, in the form

$$\frac{\partial c}{\partial t} = D\frac{\partial^2 c}{\partial x^2} + f(t), \tag{18}$$

where the unknown function $f(t)$ is to be determined from experimental data. The two-phase model with an irreversible internal kinetics discussed in the previous sections predicts a functional form $f(t) = f_o \exp(-kt)$, i.e. an exponential decay of $f(t)$. Data analysis can be performed starting from Eq. (18) by applying the Green function method and considering the boundary and initial conditions (11) and (12). The solution of Eq. (18) can be written in dimensionless form as

$$c(z,\tau) = \int_0^\tau \int_0^1 \mathcal{G}(z,\xi,\tau-\theta)\, g(\theta)\mathrm{d}\xi\mathrm{d}\theta, \tag{19}$$

where $\tau = tD/L^2$, $z = x/L$, $g(\tau) = f(\tau L^2/D)\tau$ and

$$\mathcal{G}(z,\xi,\tau-\theta) = 2\sum_{m=1}^{\infty} \sin\left[\lambda_m(1-z)\right] \sin\left[\lambda_m(1-\xi)\right] \exp\left[-\lambda_m^2(\tau-\theta)\right], \tag{20}$$

with $\lambda_m = (2m-1)\pi/2$. Correspondingly,

$$M_\tau = D\int_0^\tau \left(-\frac{\partial c}{\partial z}\right)\Big|_{z=1} \mathrm{d}\theta = \int_0^\tau \mathrm{d}\theta \int_0^\theta \mathcal{G}_1(\theta-\eta)\, g(\eta)\mathrm{d}\eta \tag{21}$$

where

$$\mathcal{G}_1(\theta) = 2D\sum_{m=1}^{\infty} \exp\left(-\lambda_m^2\theta\right). \tag{22}$$

Starting from Eq. (21) it is possible to interpolate the experimental data by developing $g(\tau)$ in power series

$$g(\tau) = \sum_{h=0}^{\infty} g_h \tau^h \tag{23}$$

and by minimizing the least-square metrics

$$\int_0^{\tau^*} \left[M_\tau - \sum_{h=0}^{N} g_h \phi_h(\tau)\right]^2 d\tau = \min, \tag{24}$$

where

$$\phi_h(\tau) = \int_0^\tau \mathrm{d}\theta \int_0^\theta \mathcal{G}_1(\theta-\eta)\eta^h \mathrm{d}\eta. \tag{25}$$

By applying least-square fitting, the unknown coefficients $\{g_h\}$ can be obtained by solving the linear system

$$\Phi \underline{g} = \underline{m}, \tag{26}$$

where $\Phi = \{\Phi_{hk}\}$ is a $(N+1)\times(N+1)$ matrix,

$$\Phi_{hk} = \int_0^{\tau^*} \phi_h(\tau)\,\phi_k(\tau)\mathrm{d}\tau, \tag{27}$$

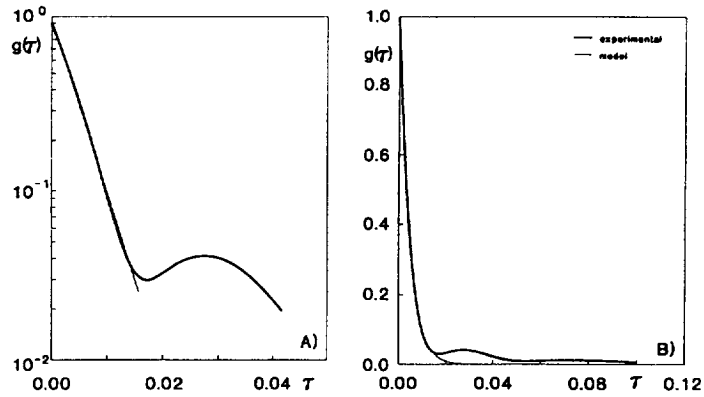

Fig. 11. (A) Log normal plot $g(\tau)$ vs. τ. The line highlights the exponential nature of $g(\tau)$ and the slope is proportional to the value of k. (B) Comparison of $g(\tau)$ with the exponential fitting with $k = 233 \cdot 10^{-3}$ s^{-1}.

$\underline{g} = (g_0, \ldots, g_N)$, and $\underline{m} = (m_0, \ldots, m_N)$ is a $(N+1)$-dimensional vector associated with the experimental measurements of the release M_τ

$$m_h = \int_0^{\tau^*} M_\tau \phi_h(\tau) \mathrm{d}\tau. \tag{28}$$

In the optimization of the least-square functional (24) the order of polynomial N and the time-instant τ^* are to be specified. The optimization procedure is not affected by the value of N as it is sufficiently large ($N > 8$). The value of τ^* is more important since, for high Thiele moduli, it should be selected in order to enhance the initial release behaviour. We chose τ^* as the value of dimensionless time furnishing a fractional release of 0.35, i.e. $M_\tau \cdot / M_\infty = 0.35$. However, the numerical evaluation of the coefficients $\{g_h\}$ is robust for small changes in $0.25 \leq M_\tau \cdot / M_\infty \leq 0.45$.

Fig. 11A and B shows the results of optimization together with the exponential fitting with $k = 2.3 \cdot 10^{-3}$ s^{-1} ($N = 19$). The exponential behaviour of $g(\tau)$ is in agreement with the two-phase model predictions, and the obtained value of k is of the same order of magnitude as the short-cut estimate discussed in the previous section. The small quantitative discrepancy between the values of k obtained here and in the previous section is of minor relevance, especially if we consider that for $k = 2.3 \cdot 10^{-3}$ s^{-1} and $D = 6.0 \cdot 10^{-6}$ cm^2/s, from the curve of Fig. 7A we obtain a value of $n = 0.60$, which is within the error range of the experimental estimate of n.

8. Conclusions

This article presents experimental results of the release of theophylline from water-swollen scleroglucan matrices which show a value of the exponent n that is definitely larger than 1/2. The predictions of the two-phase model proposed prove to be in close agreement with the experimental results.

We also present a simple approach for parameter identification from release data. From the scaling of the fractional release it is possible to obtain an accurate value of the solute diffusivity D. From the value of exponent n, given D, the value of the parameter k can be easily estimated. In particular, the dependence of n on k and D is extremely interesting since it enables to understand the role of the Thiele modulus Φ in apparent anomalies in release kinetics.

The anomalous exponent n observed in release systems with a constant swelling degree is a monotonic decreasing function of Φ^2.

The model results have been also checked with literature data on the controlled release of theophylline from HEMA-GMA matrices [3].

The analysis presented opens up interesting research perspectives in the study of controlled release through swollen gels. The microscopic interpretation of origin of the entrapped phase as a consequence of specific solute/matrix interactions is certainly the most interesting topic to be investigated. It is also important to compare the predictions of the proposed two-phase model with other models that introduce a time-dependent diffusion coefficient to take into account the dependence of the diffusivity on the swelling degree, in those cases in which the swelling degree varies appreciably during the experiment. These topics constitute the main thrust of our present research activity.

9. List of symbols

A	lab surface area
A_s	effective release area
$b(\varphi,n_0)$	see Eq. (8)
c	drug concentration
$\bar{c}$	dimensionless drug concentration in the sol phase
c_0	initial drug concentration
D	effective diffusion coefficient
D_E	Stokes–Einstein diffusivity
G	accessibility factor
$\mathcal{G}$	Green Function
k	kinetic coefficient
L	gel slab thickness
M_t/M_∞	fractional solute release
M_τ	solute release up to the dimensionless time τ
n	anomalous exponent [see Eq. (1)]
N	order of polynomial expansion
n_0	number of net holes
q	drug concentration in the gel phase
$\bar{q}$	dimensionless drug concentration in the gel phase
s	swelling degree
s_0	initial swelling degree
t	time
T	temperature
x	spatial coordinate
z	dimensionless spatial coordinate

9.1. Greek letters

ϵ_s	initial drug partition coefficient between the sol and the gel phase
λ_m	$(2m-1)\pi/2$ (see Eq. (20))
μ_m	see Eq. (14)
$\mu_{m\infty}$	see Eq. (15)
τ	dimensionless time
τ^*	see Eq. (27)
φ	A_s/A
Φ	Thiele modulus
ϕ_h	see Eq. (25)

Acknowledgements

The authors thank V. Dovi for useful suggestions and discussions. The research was performed on behalf of VectorPharma.

References

[1] P.L. Ritger and N.A. Peppas, A simple equation for description of solute release II. Fickian and anomalous release from swellable devices, J. Controlled Release, 5 (1987) 37.
[2] J. Hadgraft, Calculation of drug release rates from controlled release devices, the slab, Int. J. of Pharmac., 2 (1979) 177.
[3] N.R. Vyavahare, M.G. Kulkarni and R.A. Mashelkar, Zero order release from swollen hydrogels, J. Membrane Sci., 54 (1990) 221–228.
[4] J.S. Vrentas, C.M. Jarzebski and J.L. Duda, A Deborah number for diffusion in polymer–solvent systems, AIChE J., 21(5) (1975) 894.
[5] A. Adrover, M. Giona and M. Grassi, Analysis of controlled release in disordered structures: a percolation model, J. Membrane Sci., in press.
[6] R.A. MacDonald, Modelling macromolecular diffusion through a porous medium, J. Membrane Sci., 68 (1992) 93.
[7] W.M. Deen, Hindered transport of large molecules in liquid-filled pores, AIChE J., 33 (19??) 1409.
[8] C.T. Reinhart and N.A Peppas, Solute diffusion in swollen membranes. Part II. Influence of crosslinking on diffusive properties, J. Membrane Sci., 18 (1984) 227.
[9] P.I. Lee, Kinetics of drug release from hydrogel matrices, J. Controlled Release, 2 (1985) 277.